PHYSICAL REVIEW B **85**, 060502(R) (2012)

Size-induced melting and reentrant freezing in fullerene-doped helium clusters

F. Calvo

LASIM, Université Claude Bernard Lyon 1 and CNRS UMR 5579, 43 Bd du 11 Novembre 1918, F69622 Villeurbanne Cedex, France

(Received 16 September 2011; revised manuscript received 27 January 2012; published 6 February 2012)

The structural and dynamical stabilities of $C_{60}^+He_N$ clusters are theoretically investigated using global optimization and path-integral simulation methods. Up to $N = 32$, the fullerene ion traps the helium atoms onto sixfold and fivefold faces, strongly enough to negate vibrational delocalization. Above this size, geometric frustration takes over and the clusters grow as a thin but homogeneous liquid layer. However, as their size reaches 60 atoms, corrugation barriers are suppressed and the cluster is again rigidlike. Additional fluid layers are predicted to arise above 72 atoms.

DOI: 10.1103/PhysRevB.85.060502 PACS number(s): 67.90.+z, 36.40.Mr, 61.46.Bc

The physics and chemistry of ordinary matter can strongly vary and show intriguing phenomena upon cooling, such as superconductivity, resonance, or tunneling effects. Decreasing the number of constituents down to the nanoscale regime provides another way of modifying the properties, most often quantitatively but sometimes qualitatively, as in the progressive appearance of metallicity in mercury[1] or magnesium[2] clusters. By combining the two effects of temperature and size reduction, helium droplets offer a unique cryogenic medium in which quantum effects can be particularly salient. These exceptional conditions have been exploited to achieve high-resolution spectroscopy experiments of molecular dopants[3] and to characterize, only recently, the properties of the elusive helium dimer.[4]

Beyond nanodroplets, helium films have also attracted a lot of attention in low-dimensional physics.[5,6] In the case of graphite, helium films were found to adapt as a commensurate solid,[7] whereas the lower interaction of graphene seems to make the liquid form as likely.[8] Similarly, impurities in ^{4}He droplets were found to have the ability of suppressing the superfluid property, at least in their vicinity.[9]

Based on spectroscopic measurements and dedicated calculations, it is generally accepted that a molecular dopant surrounded by too few helium atoms tends to form a complex,[10,11] a fluid droplet nucleating and growing indefinitely above some typical size. Fullerenes and nanotubes are particularly interesting types of dopant, bridging the gap between aromatic molecules and highly organized, infinite graphene. Previous theoretical studies[12,13] suggest that fullerenes as small as C_{20} bind helium strongly enough to form solid layers, eventually surrounded by fluid layers upon adsorption of extra atoms. In this Rapid Communication, we theoretically predict in the case of C_{60}^+ that the organization of helium atoms around the fullerene critically depends on their number, the helium clusters exhibiting a partial or complete fluid character if their size exceeds 32 atoms. However, around the size of 60 atoms, the clusters become rigidlike again. We show that such a reentrant behavior is intimately related to the quantum mechanical nature of helium, and is the consequence of a subtle interplay between the fullerene corrugation and the competition between the helium-fullerene and helium-helium interactions.

We have investigated the stable structures and dynamics of $^4He_N C_{60}^+$ clusters (simply denoted as $C_{60}^+He_N$ in the following), cations being preferred over neutrals for the purpose of experimental characterization. Our study relies on molecular modeling using carefully constructed or chosen interatomic potentials. We first reasonably assume that the temperature imposed by helium is low enough to keep the fullerene ion, taken as the icosahedral buckminsterfullerene isomer, as a rigid solid in its vibronic ground state. The interaction between a single He atom and the C_{60}^+ cage is modeled by considering the dominant contributions of short-range Pauli repulsion, long-range dispersion, induction, and polarization forces due to the electrostatic multipole. This interaction is described by a simple sum of pair potentials, plus a vectorial polarization term as

$$V = \sum_{i \in C_{60}} A \exp(-b r_{i0}) - \frac{C_6}{r_{i0}^6} - \frac{C_8}{r_{i0}^8} - \frac{1}{2}\alpha_{He}\vec{E}_0^2, \qquad (1)$$

where r_{i0} is the distance between atom i and the helium atom, $\vec{E}_0$ is the electric field vector at the helium site created by the molecular ion, and α_{He} is the atomic polarizability of helium. Partial charges $q_i = e/60$ on C_{60}^+ were placed on each carbon atom, in addition to 90 partial charges that best reproduce the lowest multipoles of a neutral fullerene.[14] The C_{60}^+-He potential contains five parameters which were optimized in order to reproduce the adsorption energy (16.2 meV) and equilibrium distance (6.5 Å) of the neutral system, as recently determined by Varandas from high-level quantum chemistry methods.[15,16] The He-He interaction was taken as the accurate ten-parameter Janzen-Aziz potential,[17] who fitted energy curves obtained by Korona and co-workers[18] via symmetry-adapted perturbation theory. Owing to the low polarizability of helium, the many-body effects arising between the induced dipoles were safely neglected.

The relatively high binding energy (16.8 meV) of helium atom to C_{60}^+ predicted by this model supports the formation of solid, localized structures, and we first explored the potential energy surfaces of $C_{60}^+He_N$ clusters by means of global optimization in the classical and simple harmonic quantum pictures. The most stable structures were located by basin-hopping minimization in the size range $1 \leqslant N \leqslant 100$. For each size, the harmonic zero-point-energy (ZPE) correction was also evaluated for all isomers, and the most stable resulting isomer was identified. Figure 1 illustrates the remarkable geometries found for some sizes.

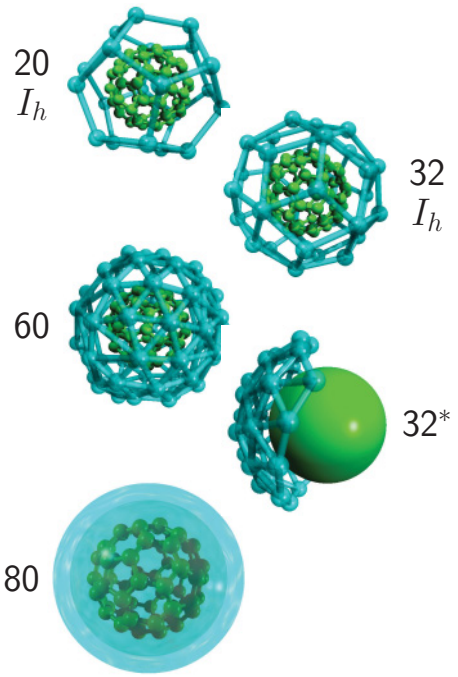

FIG. 1. (Color online) Selected structures of $C_{60}^+He_N$ clusters: icosahedral global minima for $N = 20$ and 32, nonsymmetric structure found $N = 60$ after including zero-point energy corrections, segregated structure found for $N = 32$ with the isotropic C_{60}^+-He interaction, and typical fluid structure obtained for $N = 80$.

The present interaction potential predicts a simple growing pattern for the helium atoms, which tend to localize onto neighboring hexagonal faces of the fullerene. This leads to a dodecahedron at size $N = 20$ and is followed by the filling of the pentagonal faces, reaching completion at size $N = 32$, also of the I_h point group. These results are consistent with the commensurate structure found by Kwon and Shin[13] for $C_{20}He_{32}$. Above this size, the additional helium atoms are incommensurate with the fullerene, but the defects remain within a single layer of increasing radius. Only as the number of helium atoms exceeds 72, a second layer is formed.

Upon including harmonic zero-point effects, this growing pattern is not drastically altered until size 32 is reached, except for the precise location of filled faces of a given type. However, above this size the number of He-He interactions increases, making a significant contribution to the ZPE. Structural changes induced by vibrational delocalization[19] then become more systematic, even though the quantum global minimum does not exhibit very different geometrical features.

The molecular structure of the fullerene thus seems essential in explaining these stable structures, and indeed very different results are obtained if corrugation is neglected. The C_{60}^+-He potential obtained by spherical averaging was fitted with a similar form as Eq. (1), the distance r_{i0} to a carbon atom being replaced by the effective distance $r_{i0} - R$, with the radius R of the fullerene taken as a parameter.[20] Repeating global optimization using this isotropic radial interaction leads to fully segregated helium clusters, as illustrated in Fig. 1, with the most stable structure found for $C_{60}^+He_{32}$. Interestingly, the onset of a second helium layer occurs at $N = 78$, not far from the value obtained with the atom-atom potential.

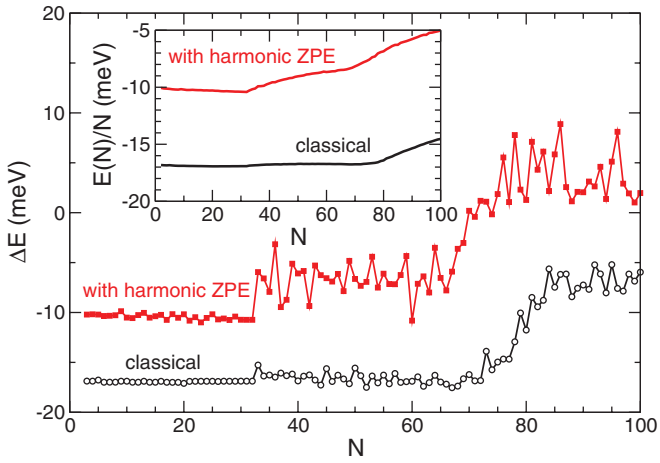

FIG. 2. (Color online) First energy difference $\Delta E(N) = E(N) - E(N-1)$ for classical and harmonic quantum $C_{60}^+He_N$ clusters. The inset shows the binding energy per helium atom.

Several of these structural results can be rationalized based on simple energetic arguments, and we show in Fig. 2 the variations of the binding energy $E(N)/N$ per helium atom, as well as the first energy difference $\Delta E(N) = E(N) - E(N-1)$, both with and without the harmonic ZPE correction. It is important to note here that the He_2 well depth amounts to only 1 meV in the Janzen-Aziz potential.[17]

As judged from the variations of ΔE and E/N, the classical system does not show special stabilities in the range of 1–80 atoms. In particular, the binding energy provided by each new atom up to size 32 is approximately constant and amounts to 16.8 meV, which is the C_{60}^+-He binding at equilibrium. The adsorption of helium on sixfold faces is slightly favorable (by about 2 meV) with respect to adsorption on pentagonal faces, and this suffices to fully explain the growth pattern up to size 32, especially the intermediate dodecahedral structure at $N = 20$.

The irregular variations of the binding energy above $N = 32$ are consistent with the formation of incommensurate defects on the helium monolayer. In this regime, interactions between helium atoms contribute to decreasing the magnitude of the average binding energy, but the effect is barely visible unless ZPE corrections are included. The two-dimensional helium monolayer cannot accommodate more than six nearest neighbors in a hexagonal close-packed fashion. Therefore the nearly constant classical binding energy indicates that each additional helium atom remains mostly bound to the C_{60}^+ ion in the vicinity of the potential energy minimum, a slight decrease in the fullerene-helium energy being compensated by some gain in the helium-helium binding contribution.

As anticipated by the more numerous He-He interactions, harmonic quantum ZPE corrections contribute significantly to the binding energy above size 32, and even more above $N \sim 65$, where ΔE becomes positive. This unphysical result is caused by the harmonic approximation, which is not expected to be accurate for helium-dominated systems. The first energy difference has a clear minimum at $N = 60$ once ZPE corrections are included, but the corresponding structure depicted in Fig. 1 does not show any special symmetry.

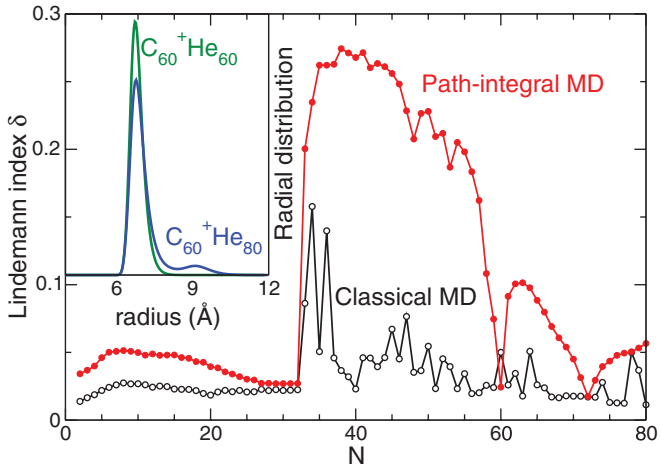

FIG. 3. (Color online) Root-mean-square bond-length fluctuations index between helium atoms in molecular dynamics simulations of $C_{60}^{+}He_N$ clusters as a function of N. Open and full symbols are the results of classical and path-integral trajectories, respectively, the temperature being set to 1 K. The inset shows the helium radial distribution functions obtained from PIMD trajectories for $N = 60$ and $N = 80$.

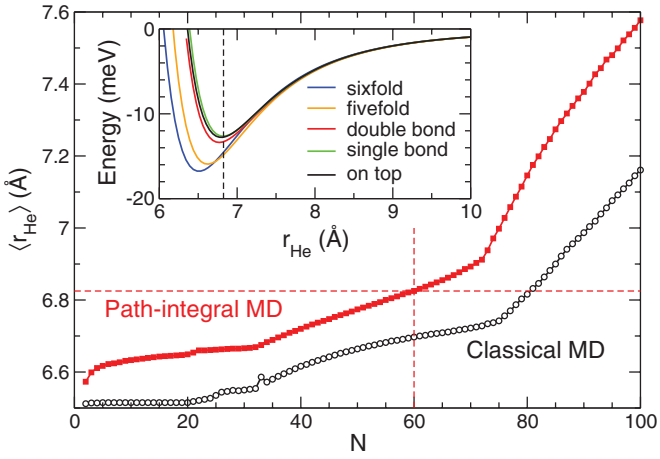

FIG. 4. (Color online) Average distance $\langle r_{He}\rangle$ from helium atoms to the fullerene center in classical (open symbols) and path-integral (full symbols) molecular dynamics simulations. The dashed lines highlight the value for $N = 60$ and $\langle r_{He}\rangle = 6.825$ Å. The inset shows C_{60}^{+}-He radial potential energy curves along several directions, with the vertical dashed line located at 6.825 Å.

The failure of the harmonic approximation displayed by the binding energies in larger clusters suggests that vibrational delocalization requires a more rigorous quantum mechanical treatment of nuclear motion, which for such relatively large systems is conveniently provided by path-integral molecular dynamics (PIMD).[21] In the present work we found a satisfactory convergence with a Trotter discretization number of $P = 32$ at $T = 1$ K. Briefly, PIMD simulations were performed by propagating the equations of motion of the original and extended system in normal mode coordinates, over a time of 10 ns with a time step of 5 fs and starting from the classical global minimum. As in the optimization process, the fullerene ion was kept rigid. Evaporation was circumvented by enclosing the system into a soft-walled container acting on helium atom j at distance r_j from the fullerene center through the repulsive potential $V_{rep}(r_j) = \kappa(r_j - R)^4\Theta(r_j - R)$, Θ being the Heaviside step function, $R = 12.5$ Å a fixed radius, and $\kappa = 10^{-2}$ eV/Å^4. Classical trajectories with $P = 1$ were also conducted under the same conditions.

Although anharmonic zero-point energies can be estimated by path-integral methods,[22] the PIMD approach was used for getting some direct insight into the rigid or fluid character of the cluster. Toward this end we computed the root-mean-square bond length fluctuation δ (also known as the Lindemann index) averaged over all pairs. In the path-integral representation, the distances were measured between centroids. The variations of δ with cluster size are represented in Fig. 3 for the classical and quantum simulations.

The Lindemann index is nearly always below 10% in the classical system, except at sizes 33 and 35, and it fluctuates somewhat above $N = 40$. Inspection of the MD trajectories confirms that the helium atoms behave essentially as a solidlike two-dimensional layer, except for localized defects either within this layer ($N \leqslant 72$) or possibly over it as floating atoms ($N > 72$).

The dynamics in the more realistic quantum mechanical systems is rather similar until the icosahedral layer is complete at $N = 32$, although the extra vibrational fluctuations due to zero-point effects are manifested by a clearly higher Lindemann index. For N above 32, our classical results agree with the recent MD results of Leidlmair and co-workers,[23] who found the majority of helium atoms to behave as solidlike. In contrast, including quantum effects leads to a much stronger disorder, the helium layer behaving as a homogeneous fluid. The Lindemann index sharply decreases as the number of helium atoms reaches $N = 60$, at which size the cluster is again rigidlike. Also surprisingly, the variations in the Lindemann index show a further increase and a maximum at $N = 64$ before decreasing again, reaching a second minimum at $N = 72$ and eventually increasing steadily above this size.

To interpret these puzzling features, it is insightful to consider the radial repartition, taking into account both size and quantum dynamical effects. The average radial distance $\langle r_{He}\rangle$ of helium atoms to the fullerene center of mass was calculated from the classical and PIMD trajectories, and its variations with cluster size are represented in Fig. 4.

These variations are generally monotonic, except for the $C_{60}^{+}He_{33}$ cluster for which the defect tends to be occasionally expelled away from the icosahedral layer in the classical system. Quantum zero-point effects have a significant contribution, enlarging the helium layer by more than 0.1 Å. The formation of a second layer above $N = 72$, confirmed by inspecting the radial distribution functions in Fig. 3, is associated with a steeper increase in $\langle r_{He}\rangle$, suggesting that this new layer should be fully delocalized. If we now represent the C_{60}^{+}-He potential as a function of radial distance for the five symmetry axes pointing to the hexagonal and pentagonal faces, the middle of single and double bonds, and to the top of carbon atoms, we find that the barriers (approximately 3 meV) are located close to 6.83 Å (see Fig. 4). This value is precisely reached by the average distance at the cluster size of $N = 60$.

This coincidence provides an explanation for the observed reentrant freezing. The layer of 60 atoms is radially located at a distance where all corrugation barriers are suppressed, the interaction to the fullerene ion being strong enough to freeze the helium atoms radially on the surface. Around this size, vacancies and defects lead to orientational heterogeneities and a large degree of dynamical disorder. In contrast to the size range 33–59, clusters containing between 61 and 71 helium atoms are mostly rigidlike with diffusing defects. $N = 72$ marks the capacitance of a single monolayer, with a sufficiently dense packing to induce a rigidlike behavior. Finally, above 72 atoms the additional He atoms nucleate as a delocalized fluid around this rigid monolayer.

In the absence of nuclear delocalization, the helium atoms are pinned too close to the molecular ion to have any chance of crossing the corrugation barriers, and they remain in a rigidlike state. Quantum mechanics is thus the cause for the qualitative nonmonotonic size effects found here. Our results can also be compared with calculations[7,8] and experiments[24] on helium films on graphite and graphene, where the interaction strength and corrugation both contribute to localizing the helium atoms into a commensurate solid. A very similar behavior is found here on the formation of the highly stable icosahedral layer at $N = 32$. Based on the present results, we expect $C_{60}^{+}He_N$ clusters to also show special stability at $N = 60$, which is consistent with the mass spectrometry results of Leidlmair and co-workers.[23]

The "magic number" found for 60 helium atoms is unusual, as it results from a subtle interplay between structural, energetic, dynamical and quantum effects. Obviously, a comparable analysis would hold for helium on other carbon nanostructures. For instance, the same calculations performed on the neutral fullerene indicate that the qualitative features of a fluid-localized transition followed by reentrant freezing and further delocalization are preserved, although not at the same exact transition sizes. A natural extension of the present work would thus be large nanotubes with exohedral or endohedral coverages, or increasingly large polycyclic aromatic hydrocarbons on the way to graphene. Exchange effects are expected to become more important as the weakly bound droplet nucleates at $N > 72$. Together with isotope effects, those would deserve further consideration using quantum Monte Carlo techniques as well as recent schemes for improving convergence with the Trotter number.[25]

In summary, we have theoretically modeled the structure and dynamics of fullerene-doped helium clusters and confirmed earlier suggestions that helium atoms bond strongly to the fullerene[12] and form commensurate structures.[13] Once the icosahedral shell is filled with 32 adatoms, the strongly quantum helium-helium interactions start to play a more important role. Defects and the presence of corrugation barriers induce a strong disorder, with the helium layer behaving as a liquid. However, 60 atoms are far away enough from the fullerene to suppress the barriers and install rigidity back into the cluster. The monolayer is complete at 72 atoms, above which a delocalized droplet nucleates and grows. Large $C_{60}^{+}He_N$ clusters are then predicted to form an essentially classical (localized) monolayer of approximately 72 atoms around the fullerene and a low-density homogeneous quantum fluid beyond.

The author wishes to acknowledge the regional computing center PSMN for generous allocation of resources, as well as P. Scheier for communicating related results prior to publication.

[1] K. Rademann, B. Kaiser, U. Even, and F. Hensel, Phys. Rev. Lett. **59**, 2319 (1987).
[2] P. H. Acioli and J. Jellinek, Phys. Rev. Lett. **89**, 213402 (2002).
[3] M. Y. Choi, G. E. Douberly, T. M. Falconer, W. K. Lewis, C. M. Lindsay, J. M. Merritt, P. L. Stiles, and R. E. Miller, Int. Rev. Phys. Chem. **25**, 15 (2006).
[4] R. E. Grisenti, W. Schöllkopf, J. P. Toennies, G. C. Hegerfeldt, T. Köhler, and M. Stoll, Phys. Rev. Lett. **85**, 2284 (2000).
[5] D. Cieslikowski, A. J. Dahm, and P. Leiderer, Phys. Rev. Lett. **58**, 1751 (1987).
[6] B. E. Clements, E. Krotscheck, and H. J. Lauter, Phys. Rev. Lett. **70**, 1287 (1993).
[7] M. E. Pierce and E. Manousakis, Phys. Rev. Lett. **83**, 5314 (1999).
[8] M. C. Gordillo and J. Boronat, Phys. Rev. Lett. **102**, 085303 (2009).
[9] R. N. Barnett and K. B. Whaley, J. Chem. Phys. **96**, 2953 (1993).
[10] F. Paesani, A. Viel, F. A. Gianturco, and K. B. Whaley, Phys. Rev. Lett. **90**, 073401 (2003).
[11] A. R. W. McKellar, Y. Xu, and W. Jäger, Phys. Rev. Lett. **97**, 183401 (2006).
[12] E. S. Hernandez, M. W. Cole, and M. Boninsegni, Phys. Rev. B **68**, 125418 (2003).
[13] Y. Kwon and H. Shin, Phys. Rev. B **82**, 172506 (2010).
[14] T. I. Schelkacheva and E. E. Tareyeva, Phys. Rev. B **61**, 3143 (2000).
[15] A. J. C. Varandas, Int. J. Quantum Chem. **111**, 416 (2011).
[16] Only the parameters A, b, C_6, and C_8 were free to vary during the optimization process, the polarizability being taken from the literature as $\alpha_{He} = 0.271$ Å^3. The optimized values are given by $A = 3.610$ eV, $b = 3.997$ Å^{-1}, $C_6 = 9.483 \times 10^{-3}$ eV Å^6, and $C_8 = 2.365 \times 10^{-5}$ eV Å^8.
[17] A. R. Janzen and R. A. Aziz, J. Chem. Phys. **107**, 914 (1997).
[18] T. Korona, H. L. Williams, R. Bukowski, B. Jeziorski, and K. Szalewicz, J. Chem. Phys. **106**, 1 (1997).
[19] F. Calvo, J. P. K. Doye, and D. J. Wales, J. Chem. Phys. **114**, 7312 (2001).
[20] The effective isotropic C_{60}^{+}-He interaction potential contains six parameters, which were all freely optimized to reproduce the binding energy and equilibrium distance obtained with the fully atomistic potential, resulting in $R = 8.23$ Å, $A = 166.68$ eV, $b = 3.729$ Å^{-1}, $C_6 = 0.223$ eV/Å^6, $C_8 = 2.594 \times 10^{-5}$ eV/Å^8, and $\alpha_{He} = 0.04$ Å^3. In this spherical model the electric field is created by a single charge e at the fullerene center.
[21] M. E. Tuckerman, D. Marx, M. L. Klein, and M. Parrinello, J. Chem. Phys. **104**, 5579 (1997).
[22] K.-Y. Wong and J. Gao, J. Chem. Theory Comput. **4**, 1409 (2008).
[23] C. Leidlmair, Y. Wang, P. Bartl, H. Schöbel, S. Denifl, M. Probst, M. Alcamí, F. Martín, H. Zettergren, K. Hansen, O. Echt, and P. Scheier, Phys. Rev. Lett. (to be published, 2012).
[24] D. S. Greywall and P. A. Busch, Phys. Rev. Lett. **67**, 3535 (1991).
[25] A. Pérez and M. A. Tuckerman, J. Chem. Phys. **135**, 064104 (2011).